Bioresource Technology 228 (2017) 279–289

Contents lists available at ScienceDirect

Bioresource Technology

journal homepage: www.elsevier.com/locate/biortech

Phosphomolybdic acid and ferric iron as efficient electron mediators for coupling biomass pretreatment to produce bioethanol and electricity generation from wheat straw

Yi Ding [a,1], Bo Du [a,1], Xuebing Zhao [a,b,*], J.Y. Zhu [c], Dehua Liu [a,b]

[a] Institute of Applied Chemistry, Department of Chemical Engineering, Tsinghua University, Beijing 100084, China
[b] Tsinghua Innovation Center in Dongguan, Dongguan 523808, China
[c] USDA Forest Service, Forest Products Lab, 1 Gifford Pinchot Dr, Madison, WI 53726, USA

HIGHLIGHTS

- Increasing biomass digestibility by phosphomolybdic acid pretreatments.
- Good hydrolyzability and fermentability were obtained.
- Re-oxidation of reduced phosphomolybdic acid for electricity generation.
- Coupling bioethanol production and electricity generation from biomass.
- Iron (III) as an efficient mediator for electron transfer in cathode reaction.

GRAPHICAL ABSTRACT

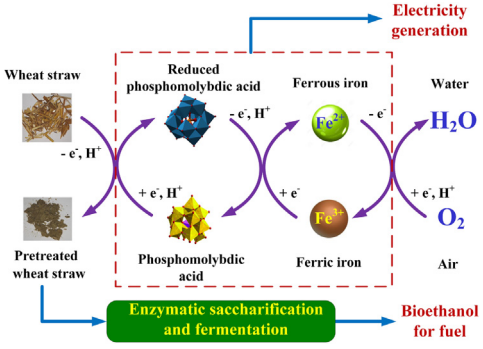

ARTICLE INFO

Article history:
Received 19 November 2016
Received in revised form 29 December 2016
Accepted 30 December 2016
Available online 3 January 2017

Keywords:
Lignocellulosic biomass
Pretreatment
Enzymatic hydrolysis
Direct lignin-to-electricity conversion
Phosphomolybdic acid
Electron mediator

ABSTRACT

Phosphomolybdic acid (PMo_{12}) was used as an electron mediator and proton carrier to mediate biomass pretreatment for ethanol production and electricity generation from wheat straw. In the pretreatment, lignin was oxidized anaerobically by PMo_{12} with solubilization of a fraction of hemicelluloses, and the PMo_{12} was simultaneously reduced. In an external liquid flow cell, the reduced PMo_{12} was re-oxidized with generation of electricity. The effects of several factors on pretreatment were investigated for optimizing the conditions. Enzymatic conversion of cellulose and xylan were about 80% and 45%, respectively, after pretreatment of wheat straw with 0.25 M PMo_{12}, at 95 °C for 45 min. $FeCl_3$ was found to be an effective liquid mediator to transfer electrons to air, the terminal electron acceptor. By investigating the effects of various operation parameters and cell structural factors, the highest output power density of about 11 mW/cm^2 was obtained for discharging of the reduced PMo_{12}.

1. Introduction

Lignocellulosic biomass has been considered as one of the most promising renewable feedstock in a biorefinery to produce energy and chemicals. Typically, woody biomass contains 40–42% cellulose, 20–30% hemicelluloses and 25–32% lignin, whereas agricultural lignocellulose contains approximately 30–40% cellulose,

* Corresponding author at: Institute of Applied Chemistry, Department of Chemical Engineering, Tsinghua University, Haidian District, Beijing 100084, China.
E-mail address: zhaoxb@mail.tsinghua.edu.cn (X. Zhao).
[1] Both authors contributed equally to this work.

http://dx.doi.org/10.1016/j.biortech.2016.12.109
0960-8524/

20–30% hemicelluloses, and 15–30% lignin (Zhu and Pan, 2010; Zhao et al., 2012a). In a typical cellulosic ethanol plant, cellulose and hemicelluloses are converted to ethanol, while the enzymatic residue rich-in lignin is burnt in a boiler to produce steam for utility or driving steam turbine for electricity generation (Lynd, 1996). However, this manner of lignin-to-electricity conversion usually causes a great loss of exergy, especially for the burning process (Amirabedin and McIlveen-Wright, 2013). On the other hand, lignin plays as a physical barrier to limit the accessibility of cellulose to cellulase enzymes (Zeng et al., 2014), and it also irreversibly and non-productively adsorb cellulase enzymes, reducing the hydrolysis efficiency of cellulose (Akimkulova et al., 2016). Therefore, by removing lignin from cell wall, cellulose accessibility can be substantively improved (Ding et al., 2012).

An idea thus comes into the mind that if oxidizing lignin for biomass pretreatment can be combined with convention of this biomass to electricity using fuel cell technology, it would achieve a co-production of biofuel (bioethanol) together with generation of electricity from biomass as proposed in the previous work (Zhao et al., 2016). However, the most important aspect of this integration is to find an efficient catalyst for delignification and electron transfer from biomass (lignin) to the oxidant. Previous works have shown that polyoxometalates (POMs), particularly phosphomolybdic acid (PMo_{12}), are good catalyst for pulp bleaching under both aerobic and anaerobic conditions, because they generally have higher redox potential than the lignin structures, so that they can oxidize the lignin, and potentials lower than oxygen, allowing their possible re-oxidation by oxygen (Gaspar et al., 2007). PMo_{12} is one of the typical Keggin type POMs with wide applications (Katsoulis, 1998). Being similar to other POMs, PMo_{12} has distinct properties such as robust oxidative degradation ability and acidity, and great potential as an electron reservoir. It has been found that PMo_{12} can be used as a good electron mediator in a novel direct biomass fuel cell that can be directly powered with natural polymeric biomasses, such as starch, for electricity generation at low temperatures (Liu et al., 2014a,b; Wu et al., 2016; Zhao and Zhu, 2016). However, noble metal catalyst such as Pt has to be used to facilitate the cathodic reaction when air or oxygen is directly used as the oxidant for discharging of the reduced PMo_{12}. The obtained power output is also relatively low. Liquid catalysts such as POMs also can be used as the electron mediator in the cathode, which greatly improves the power output (Liu et al., 2014a,b; Zhao and Zhu, 2016). To achieve a high efficiency with practical application feasibility, the cathodic mediator should be cheap and easy to re-oxidize by cheap oxidant such as air. In this work, an integrated process was proposed by coupling biomass pretreatment to increase cellulose digestibility for bioethanol production and efficient conversion of lignin to electricity using PMo_{12} as the proton and electron mediators in the anode reactions (Fig. 1). Biomass components, especially lignin was oxidized by PMo_{12} anaerobically and the reduced PMo_{12} (PMo_{12red}) were re-oxidized in a liquid flow fuel cell with electricity generation. Cheap catalyst such as Fe^{3+} was screened as the cathodic catalyst to facilitate electron transfer to air (oxygen). Such combination of biomass pretreatment and electricity generation was firstly proposed in previous work (Zhao et al., 2016), which was focused on the conception of this integrated process. The objective of this work was thus to investigate the effects of several factors on pretreatment and electricity generation, and optimize the operation parameters in terms of anaerobical pretreatment of lignocellulosic biomass (wheat straw) by PMo_{12} to improve cellulose hydrolyzability and discharging of the reduced PMo_{12} for electricity generation. The obtained data may serve as a step for further optimizing, evaluating and intensifying this novel integrated process.

2. Materials and methods

2.1. Chemicals and biomass materials

Wheat straw (WS) harvested in Shandong province, China, was used as a representative lignocellulosic biomass. It was chopped to about 1 cm long prior to PMo_{12} pretreatment. All chemicals mainly including phosphomolybdic acid ($H_3PMo_{12}O_{40}$, PMo_{12}), H_3PO_4, H_2SO_4, acetic acid, $FeCl_3$, $Fe_2(SO_4)_3$ and $Fe(NO_3)_3$ were reagent grade and purchased locally. Cellulase (Cellic® CTec2) was kindly provided by Novozymes (Beijing branch), which was a multi-enzymes formulation having a determined cellulase activity (filter paper activity, FPA) of 114.07 FPU/mL. This cellulase formula also contains xylanase to hydrolyze xylan of the substrates. The proton exchange membranes (PEMs) used for discharging of reduced POMs were Nafion®115, Nafion®117 and Nafion®212 (DuPont™, USA). Graphite bipolar plate was purchased from Hunan Jiangnan Graphite Co., Ltd (Changsha, China).

2.2. PMo_{12} pretreatment of wheat straw

PMo_{12} pretreatment of wheat straw were performed in a stirred stainless steel autoclave with an electric heating jacket (pretreatment temperature $\geqslant$100 °C) or in a round-bottom flak immerged in water bath (pretreatment temperature <100 °C). Typically, when POM was used for anaerobic delignification, the temperature and POM concentration used in laboratory experiments were in the range 100–125 °C and 0.05–0.5 mol/L, respectively (Gaspar et al., 2007). However, in the present work, since more lignin was present in the raw biomass feedstock, and thus a broader range of reaction temperature (90–160 °C) was investigated. In details, 5 g of chopped wheat straw was put in the autoclave or flask followed by addition of 50 ml 0.1–0.25 M PMo_{12} solution and 0–0.15 M H_3PO_4. The pretreatment was performed for 15–60 min. After the pretreatment, the solid was filtered and the filtrate was analyzed for reduction degree of PMo_{12}. The solid was then washed roughly by running water until neutrality followed by washing with 95% ethanol and ether successively for twice, respectively, to remove the residual PMo_{12} as much as possible. One part of the solid was dried for chemical component analysis, and the other part was store at 4 °C for enzymatic hydrolysis.

2.3. Enzymatic hydrolysis of pretreated wheat straw

The solid substrates were incubated at 50 °C, 150 rpm in 50 mM sodium acetate buffer (pH 4.8) in an air-bath shaker. All experiments were performed in duplicate with 10 mL working volume at initial solid consistency of 2.5% (g/ml) with cellulase loading of 15 FPU/g solid for 72 h. Sample were withdrawn at regular intervals and diluted for 10 folds to determine cellobiose, glucose and xylose concentrations. Enzymatic digestibility was characterized by enzymatic glucan conversion (*EGC*, %), defined as the percentage of glucan converted to glucose and cellobiose as the following equation:

$$EGC\ (\%) = \frac{C_g + C_c}{s \times 1.1 \times G_{ln}} \times 100\% \quad (1)$$

where C_g and C_c are the concentrations of glucose and cellobiose in the enzymatic hydrolysate, respectively, g/L; s is the initial solid loading in the system, g/L; G_{ln} is the glucan content of the substrate.

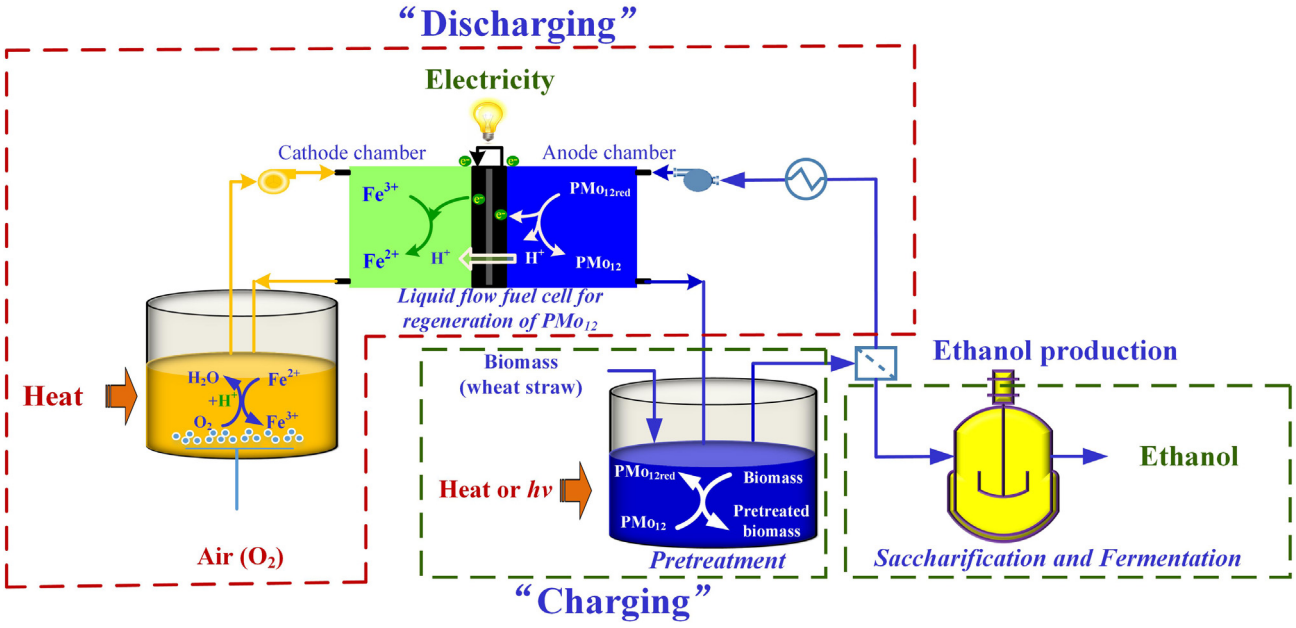

Fig. 1. A conceptual integration of PMo_{12}-mediated biomass pretreatment for ethanol production and electricity generation.

2.4. Semi-simultaneous scarification and fermentation for ethanol production

Semi-simultaneous scarification and fermentation (sSSF) was carried out in 25 mL Erlenmeyer flasks with total working volume of 10 mL with an air shaker incubator at 150 rpm with 5–15% (w/v, g/mL) solid substrate loading. Other nutrients including 2 g/L $(NH_4)_2SO_4$, 5 g/L KH_2PO_4, 5 g/L yeast extract, 1 g/L $MgSO_4$ and 0.2 g/L $CaCl_2$ dissolved in pH 5.3 H_2SO_4 solution was then added in order to obtain an initial pH of about 5.2–5.4 in the sSSF system. The mixture was autoclaving at 121 °C for 20 min for sterilization. After the mixture was cooled down to room temperature, the cellulase enzymes of 20 FPU/g solid were added. The mixture was then incubated at 50 °C for pre-hydrolysis for 24 h followed by inoculation of yeast *Saccharomyces cerevisiae* (Angel Yeast Co., Ltd, China) for fermentation for 48 h. Samples were taken every 6, 12 or 24 h for analyzing ethanol and sugar concentrations. The ethanol yield was calculated according to ethanol concentration and expressed as the percentage of theoretical maximum ethanol yield (Chen et al., 2015).

2.5. Assembly of the cell

The strucure of the liquid flow fuel cell was similar to that used in the previous work (Zhao and Zhu, 2016; Zhao et al., 2016). The cell is composed of two graphite bipolar plates as anodic and cathodic electrodes, respectively. The inner side of each bipolar plate had several 2 mm-wide and 2 mm-deep flow channels with total active area of 0.7–35.2 cm^2. A PEM was sandwiched between the two bioplar plates to separate the cell into an anode chamber and an cathode chamer. These biopolar plates and MEA were further sandwiched by two acrylic plastic end plates. Silicone rubber gasket was used between bioplar plate and PEM to prevent leakage. The anode or cathode chamber were connected by Teflon and silicone pipes with external anode and cathode vessels containning reduced PMo_{12} and Fe^{3+}, respectively. The anode vessel worked as a biomass pretreatment rectors. The working principle of the system are described as follows. In the anode vessel, chopped wheat straw was pretreated by PMo_{12} anaerobically, in which oxidation of lignin was the main oxidative reaction with PMo_{12} being reduced to form reduced PMo_{12} (PMo_{12red}) and a fraction of hemicelluloses was also hydrolyzed. Due to the hydrolysis of hemicelluloses and oxidative delignification, the pretreated solid was susceptible to enzymatic saccharification and fermentation for ethanol production. Electrons and protons transferred from lignin to PMo_{12} as shown in Eq. (2). Heat or light can be used to accelerate the reaction. In the anode chamber, PMo_{12red} released electrons and protons, and was re-oxidized to PMo_{12} which was further recycled to anode vessel for biomass pretreatment. In the cathode chamber, mediator such as Fe^{3+} obtained electrons to form the reduced mediator, such as Fe^{2+}. In the cathode vessel, the Fe^{2+} was further re-oxidized to Fe^{3+}, which achieved transfer of electron to final oxidant such as air (oxygen). Corresponding reactions of the process can be described as following Eqs.:

$$\text{In anode vessel}: \text{Lignin} - H_n + PMo_{12} \rightarrow \text{Oxidizedlignin} + H_n - PMo_{12red} \quad (2)$$

$$\text{In anode chamber}: H_n - PMo_{12red} \rightarrow PMo_{12} + ne^- + nH^+ \quad (3)$$

$$\text{In cathode chamber}: Fe^{3+} + e^- \rightarrow Fe^{2+} \quad (4)$$

$$\text{In cathode vessel}: O_2 + 4Fe^{2+} + 4H^+ \rightarrow 2H_2O + 4Fe^{3+} \quad (5)$$

In this integrated process, the pretreatment is a "charging" process in which electrons transfer from biomass component, mainly lignin, while in the liquid flow fuel cell the re-oxidation of PMo_{12red} is a "discharging" process to produce electricity. Therefore, this integrated process not only achieves a pretreatment of lignocellulosic biomass to increase cellulose digestibility for sugar and bioethanol production, but also achieves a direct conversion of biomass, particularly lignin, to electricity at low temperatures (Zhao et al., 2016). In the experiments, for investigating the effects of several factors on "charging" and "discharging" processes, separately, WS was first pretreated using PMo_{12}, and the reduced PMo_{12} solution was filtered from the slurry and pumped into the cell for electricity generation.

2.6. Discharging of reduced PMo_{12}

After filtration from the slurry of PMo_{12}-biomass mixture, the reduced PMo_{12} solution and liquid catalyst (Fe^{3+}) were continously circulated from anode or cathode vessels, respectively, at a flow rate of 10–100 mL/min by a peristaltic pump. The vessels were immersed in a water bath heated to a desired temperature of 25–90 °C. The cathode vessel was supplied with air or pure oxygen as final electron acceptor from a pressurized cylinder by Teflon pipes to reoxidize Fe^{2+} to Fe^{3+}. An external resistance of 2 Ω was loaded between the cathode and anode graphite felts. Voltage on the external resistance and current were determined by a VICTOR VC8245 Multimeter (Shenzhen City Health Station Victory Technology Co., Ltd, China) and CHI660E Electrochemical Workstation (Shanghai Chenhua Instrument Co., Ltd, Shanghai, China).

2.7. Analytic methods

2.7.1. Chemical compositions of wheat straw and pretreated solid

The main components of raw wheat straw and pretreated solids were determined according to NREL's Laboratory Analytical Procedure. The monosaccharaide (glucose, xylose and arabinose) concentrations were determined by Shimadzu (Tokyo, Japan) HPLC (LC-10AT) system quipped with an Aminex HPX-87H column (Bio-Rad, Hercules, CA, USA) and a differential refraction detector using 5 mM H_2SO_4 as an eluent at flow rate of 0.8 ml/min.

2.7.2. Fourier transform infrared spectroscopy (FTIR)

FTIR spectroscopic analysis was performed using a Thermo Scientific Nicolet iN10 FTIR Microscope (Thermo Nicolet Corporation, Madison, WI) equipped with a liquid nitrogen cooled MCT detector. Acetone-dried samples were embedded in KBr pellets with an approximate concentration of 1 mg/100 mg KBr. Scans were conducted at 400–4000 cm^{-1}. Before data collection, background scanning was performed for correction.

2.7.3. Crystallinity analysis

The crystallinities of wheat straw and pretreated solid were determined by X-ray diffraction (XRD) using XRD-6000 instrument (Shimadzu, Japan). The X-ray diffractograms were recorded from diffraction angle (2θ) of 5° to 50° at a scanning speed of 5°/min with Ni-filtered Cu Kα radiation (χ = 1.54 Å) at 40 kV and 40 mA. The crystallinity index (*CrI*) was calculated using the following expression: $CrI = (I_{002} - I_{am})/I_{002} \times 100\%$, where I_{002} is the intensity of peak at a 2θ angle of ~22.6° and I_{am} is the scattering intensity of amorphous fraction at a 2θ angle of ~18.3°.

2.7.4. Determination of polarization curves, reduction degree of PMo_{12}, Fe^{2+} concentration and Faraday efficiency

The polarization curves were determined by measuring voltages generated by the fuel cell when it was loaded with a variable external resistance from 1 to 10,000 Ω, and the current density was calculated by Ohm law. The output power density was then calculated by voltage and current density (Kim et al., 2004).

The reduction degree (*RD*, %) of PMo_{12} was defined as the percentage of formed Mo^{5+} on the total Mo^{5+} formed by complete reduction of Mo^{6+}. It should be noted that 1 Keggin structure of PMo_{12} can accept 8 electrons though there are 12 Mo atoms in a Keggin structure (Zhang et al., 1990). Complete reduction of PMo_{12} was obtained by using excessive ascorbic acid. Standard curve thus can be established between Mo^{5+} concentration and absorption at 860 nm (Zhao et al., 2016).

Fe^{2+} concentration was determined by phenanthroline method (Tamura et al., 1974).

Faraday efficiency (ε_F) was calculated by the following the following Eqn.:

$$\varepsilon_F = \frac{Q_{discharge}}{Q_{PMo12}} \quad (6)$$

where $Q_{Discharge}$ is the experimental charge quantity accepted by Fe^{3+} to form Fe^{2+}, and Q_{PMo12} is the charge quantity released by reduced PMo_{12} calculated by spectrophotometry.

3. Results and discussion

3.1. Pretreatment of wheat straw by PMo_{12}(the "charging" process) to increase cellulose enzymatic digestibility

3.1.1. Effects of various factors on pretreatment

Biomass pretreatment is a prerequisite step to improve the cellulose digestibility for a biorefining system to produce various derivative products (Zhu and Pan, 2010; Zhao et al., 2012b). Particularly, the presence of lignin in cell wall has been found to be an important structural factor protecting cellulose fiber from degradation (Zeng et al., 2014). Various delignification processes have been employed as a biomass pretreatment to increase cellulose accessibility such as alkaline saponification (Kim et al., 2016), oxidative delignification (Singh et al., 2014), solvent extraction (Zhao et al., 2009) and sulfite pulping (Zhu et al., 2009). However, most of the oxidants used in the oxidative pretreatment, such as O_3, H_2O_2, $NaClO_2$, are not recyclable or easily regenerated. POMs have been employed as catalysts for oxygen pulping of pulps for several decades (Gaspar et al., 2003). Nevertheless, very few research works have been found in literatures for POM pretreatment of biomass to increase cellulose digestibility. Actually, POM is very promising to use for biomass pretreatment (Zhao et al., 2016), because POM is a strong acid and oxidant and can achieve a simultaneous hydrolysis of hemicelluloses and oxidative delignification. The acidity, oxidizing ability and redox properties of POM can be easily tailored by changing the composition of the Keggin units (Kozhevnikov, 1998), and the reduced POM can be regenerated by other oxidants with higher redox potential. Different PMo_{12} concentrations were used to pretreat wheat straw under various conditions as shown in Supplemental data Table S1. Runs 1–16# is an orthogonal array design (Taguchi design) to investigate the effects of pretreatment temperature (*T*, °C), PMo_{12} concentration (C_{PMo12}, M), time (*t*, min) and external addition of H_3PO_4 (C_{H3PO4}, M) on pretreatment efficacy. Corresponding leverage profiles of different factors on various response variables including solid yield (*SY*, %), glucan content (G_{ln}, %), xylan content (X_{ln}, %), lignin content (L_{ig}, %), degree of delignification (*DD*, %), solubilizations of glucan (S_{Gln}) and xylan (S_{Xln}), enzymatic glucan conversion (*EGC*, %) and reduction degree of PMo_{12} (*RD*, %), are shown in Fig. 2A–D. Temperature demonstrated very significant effects on pretreatment as shown in Fig. 2A. *SY* decreased with increase in temperature from 100–160 °C mainly due to the solubilization of polysaccharide and lignin. Significant solubilization of glucan and xylan were observed, especially at high temperature, which could be as high as about 100% at 160 °C. However, *DD* contrarily decreased with increase in pretreatment temperature, and the same tendency was observed for the *EGC*. For example, the average *DD*s at 100, 120, 140 and 160 °C were 62.8%, 53.6%, 41.8% and 28.1%, and corresponding *EGC*s@24 h were 83.0%, 76.8%, 56.8% and 41.1%, respectively. This was probably due to the condensation of lignin that usually takes place under a strong acid condition. The cellulase formula used in the present work also contained xylanase, and therefore, hydrolysis of xylan was also observed in the enzymatic hydrolysis process. The xylan conversion was in the range of 40–90% depending on pretreatment conditions, and showed the same tendency with that of *EGC*. In terms of the *RD* of PMo_{12}, the optimal temperature was 140 °C. At high temperatures such as 160 °C, decomposition of PMo_{12}

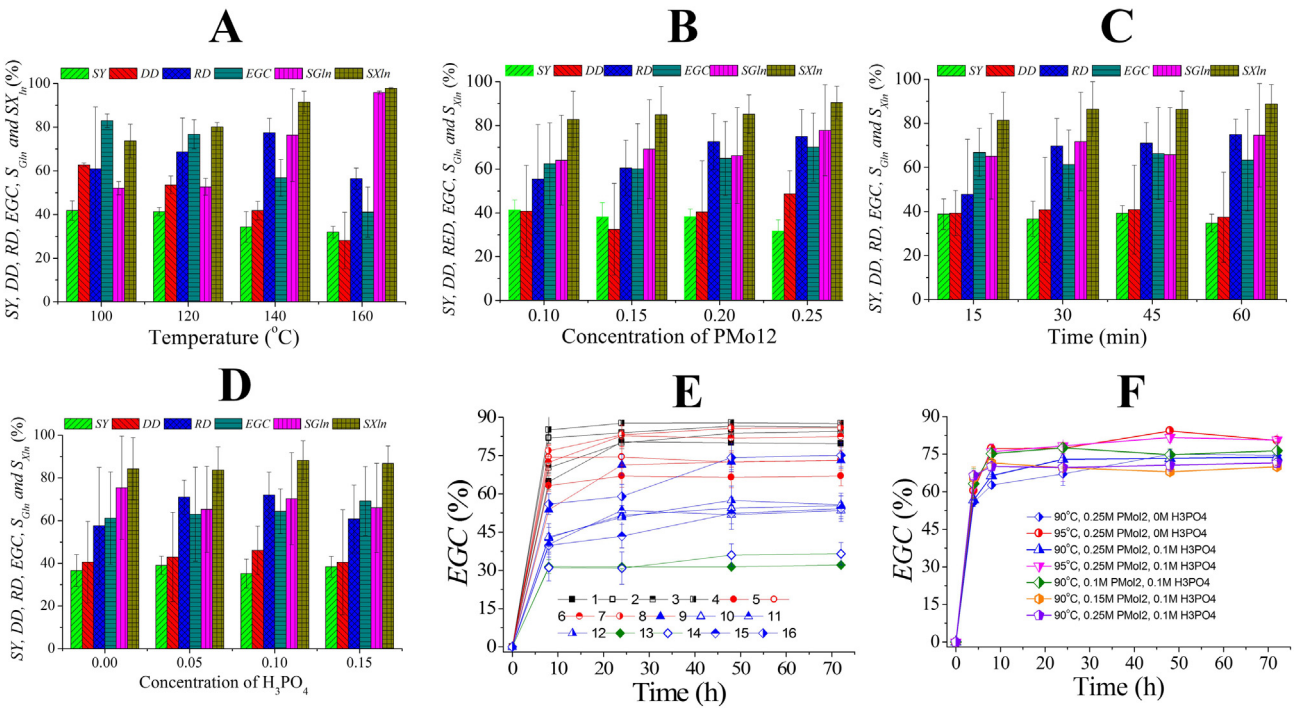

Fig. 2. Leverage profiles of different factors on various response variables during PMo_{12} pretreatment of wheat straw and corresponding enzymatic digestibility of pretreated solid. (A) Effects of temperature (*T*, °C); (B) Effects of PMo_{12} cocnentration (C_{PMo12}, M); (C) Effects of pretreatment time (*t*, min); (D) Effects of external addition of H_3PO_4 (C_{H3PO4}, M); (E) Enzymatic glucan conversion (*EGC*, %) of pretreated substrates by orthogonal array design; (F) Enzymatic glucan conversion (*EGC*, %) of substrates pretreated at lower temperatures.

might take place which reduced the *RD*. A direct evidence for this conclusion was the increase in ash content of the pretreated samples at high pretreatment temperature. It was determined that the average ash content of the pretreated solid increased from 10.4 and 9.4% at 100 °C and 120 °C to 16.2% and 26.0% at 140 °C and 160 °C, respectively. Statistical analysis indicated that *T* was the most important factors showing very significant effects on the response variables (P = <0.0001–0.0013), while C_{PMo12} also showed very significant influence on *SY* (P = 0.0058) and S_{Xln} (P = 0.0182). Other factors generally showed non-significant effects (P > 0.05), which also can be demonstrated from Fig. 2A–D that most of the response variables showed just minor changes with the increase in the levels of these factors. The highest *RD* and *EGC* were found at C_{PMo12} of 0.20–0.25 M, *t* of 30–45 min and C_{H3PO4} of 0.05–0.1 M.

The time courses of enzymatic hydrolysis of pretreated substrates by orthogonal array design shown in Fig. 2E indicated that the glucan of pretreated substrates generally could be quickly hydrolyzed within 24 h; however, prolonging hydrolysis time showed no further increase in the *EGC*. Samples obtained at 100 °C (#1–4) and 120 °C (#5–8) majorly showed much higher digestibility than those obtained at 100 °C (#9–12) and 120 °C (#13–16). These experimental results indicated that PMo_{12} pretreatment of wheat straw should be conducted at lower temperature, in order to minimize the solubilizations of glucan and lignin condensation. Therefore, experiments were further performed at lower temperatures (90 and 95 °C) with 0.1–0.2 M PMo_{12} as run #17–23 shown in Supplemental data Table S1. The results showed that *SY* increased and S_{Gln} and S_{Xln} were dramatically reduced; however, *DD* and *RD* were also greatly reduced, but *EGC* was only somewhat decreased compared with those obtained at higher temperatures. Lower PMo_{12} concentration resulted in even a slight increase in *EGC* as shown in run #21–23 of Table S1 and Fig. 2F. However, the *RD* of PMo_{12} decreased with PMo_{12} concentration, which is not beneficial for electricity generation to obtain a high power output in the liquid flow fuel cell. Therefore, with an integrated consideration, the optimal condition of PMo_{12} pretreatment of wheat straw was selected as 95 °C, 0.25 M PMo_{12} concentration, 45 min pretreatment time with 0.1 M of external addition of H_3PO_4.

3.1.2. Semi-simultaneous scarification and fermentation for ethanol production

Semi-simultaneous scarification and fermentation (sSSF) of PMo_{12}-pretreated substrates were further performed at solid loadings of 5%, 10% and 12.5%, respectively for ethanol production as shown in Fig. 3. Higher glucose concentration could be obtained at higher solid loading. After pre-hydrolysis for 24 h, glucose concentrations reached 20.4, 36.8 and 47.0 g/L at 5, 10 and 12.5% solid loadings, corresponding to 87.9, 79.3 and 81.1% of theoretical yield, respectively. After inoculation with *S. cerevisiae*, glucose concentration quickly decreased to less than 1 g/L within 12 h, and ethanol concentration generally reached the maximum of 9.92, 18.3 and 22.9 g/L, respectively, corresponding to 84.0, 77.5 and 77.6 of theoretic yields based on the cellulose in the pretreated substrate. By-product such as glycerol and acetic acid were detected in the fermentation broth, which consumed a part of the carbon source. Moreover, glucose was also consumed for cell growth to accumulate biomass. The above results indicated that the pretreated substrates showed good fermentability for ethanol production, and the obtained ethanol titer was similar to or even higher than those of reported works using dilute acid pretreatment and batch fermentation (Saha et al., 2005; Kim et al., 2011; Morikawa et al., 2014). This is mainly attributed to the good enzymatic digestibility of pretreated substrates because sugar release generally is the rate limiting step for SSF. However, it should be noted that in the present work, PMo_{12} pretreatment could be performed under mild condition (95 °C) but achieved a good cellulose conversion (~80%). Nevertheless, conventional dilute acid

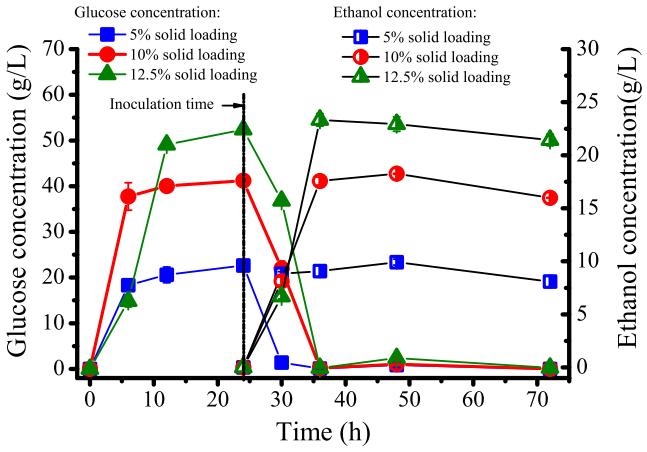

Fig. 3. Time courses of Semi-simultaneous scarification and fermentation of PMo_{12}-pretreated substrates for ethanol production.

pretreatment is usually performed at >140 °C, in order to remove a great part of hemicellulose and significantly modify lignin structure with lignin melting, migration and redistribution in cell wall (Chen et al., 2016). In this work, removal of hemicellulose were achieved by PMo_{12} pretreatment with simultaneous removing a part of lignin, thus greatly improving cellulose accessibility, because delignification under mild condition has been proved to be effective to improve cellulose hydrolysability (Ding et al., 2012; Chen et al., 2016).

3.1.3. Structural features of pretreated substrates

To further understand the mechanism of PMo_{12} pretreatment to improve cellulose digestibility, the structural features of the pretreated substrates were analyzed by SEM, FTIR and XRD as shown in Supplemental dada Fig. S1. Clear cell wall structure was observed for the raw wheat straw (Fig. S1-A) with compact and non-porous surface morphology (Fig. S1-B). After PMo_{12} pretreatment, the cell wall structure was destructed to form fine fibers with length less than 500 μm (Fig. S1-C). The substrate surface became much coarser with porous structure (Fig. S1-D), and therefore the specific surface area was greatly increased. Sphere substance was also observed, which might be produced by condensation of lignin and its re-precipitation on the fiber surface (Zhao et al., 2016; Donohoe et al., 2008). FTIR spectra (Fig. S1-E) confirmed the removal of hemicellulose (xylan) since the band at 1720 cm^{-2} which is ascribed to the acetyl groups of hemicelluloses or to the ester linkage of caboxylic streching group of ferulic acid (Morikawa et al., 2014) disappeared. The band at 1506 cm^{-2} that is attributed to the aromatic skeletal vibrations of lignin became weaker, illustrating the removal of a fraction of lignin. No more difference was found in other bands, indicating that no new chemical groups were formed during PMo_{12} pretreatment. XRD diffractograms (Fig. S1-F) demonstrated that PMo_{12} pretreatment did not alter the cellulose crystalline polymorph, and the pretreated substrates showed a typical diffractogram of natural cellulose (Cellulose I). This phenomenon was the same as those observed in many other pretreatment such as dilute acid pre-hydrolysis, steam explosion and organosolv pretreatment (Zhao et al., 2009, 2012b). The *CrI* was calculated as 38.8% for the raw wheat straw and 50.8% for the pretreated sample. This increase in *CrI* was mainly caused by removal of amorphous fractions of cellulose and lignin and hemicelluloses, as usually found in many of other pretreatment processes (Zhao et al., 2012a; Chen et al., 2016).

The above results indicated that PMo_{12} pretreatment resulted in both delignification and removal of hemicelluloses. As found in previous work (Zhao and Zhu, 2016) on structure change of lignin oxidized by PMo_{12}, the hydroxyl group content was reduced whereas the carbonyl group content increased. Both condensation and depolymerization takes place during the PMo_{12} oxidation of lignin. Significant increase in weight-average molecular weight (M_w) was observed for the oxidized kraft lignin, from 3350 (kraft lignin) to 10,080 (oxidized lignin) (Zhao and Zhu, 2016). This result further corroborated that the decrease of *DD* at high temperature was attributed to lignin condensation. Low-molecular weight phenol derivatives such as benzoic acid, p-hydroxy benzaldehyde, vanillin, acetovanillone, vanillic acid, veratraldehyde, veratric acid, syringaldehyde, acetosyringone, and 2,6-dimethoxy-p- benzoquinone were identified in the solution as degradation products (Bujanovic et al., 2010). However, complete oxidation of lignin to CO_2 and water by PMo_{12} oxidation is impossible under the pretreatment condition used in the present work since some non-phenolic moieties are difficult to oxidize by PMo_{12}. These lignin degradation and modification definitely was beneficial to expose cellulose surface for enzymatic hydrolysis. However, it should be noted that PMo_{12} are also strong acids and may result in a significant removal of hemicelluloses. Phosphoric acid was also used in the pretreatment which might also contribute to the increase in cellulose digestibility. However, a control experiment was performed with the same phosphoric acid concentration (0.25 M) at 95 °C for 45 min. This pretreatment removed about 65% of the hemicelluloses, but the obtained pretreated substrates only showed about 35% enzymatic glucan conversion. Moreover, Zhou et al. (2015) found that pretreatment of wheat straw with 5wt% (about 0.5 M) sulfuric acid at 120 °C for 1 h obtained an *EGC* of 55% at a cellulase loading of 20 FPU/g solid, which was still much lower than that obtained by PMo_{12} pretreatment. These results indicated that the improvement of cellulose digestibility by PMo_{12} pretreatment was mainly due to the deconstruction of cell wall caused by delignification as well as removal of hemicelluloses simultaneously, thus increasing the substrate surface area for cellulase binding. However, delignification seemed to be more important to exposing cellulose.

3.2. Electricity generation by re-oxidation of reduced PMo_{12} in liquid flow fuel cell

3.2.1. Effects of operational parameters

The obtained reduced PMo_{12} (0.2 M with addition of 0.36 M H_3PO_4) was discharged in a liquid flow fuel cell. Various discharging conditions were investigated to optimize the power output as shown Fig. 4. As reported in previous works (Zhao and Zhu, 2016), when air or O_2 is directly used for discharging, a noble metal such as Pt is required as a catalyst. Moreover, air or O_2 cathode usually suffers from the limitation of mass transfer because of the reaction taking place in a gas–liquid–solid tri-phase system. Therefore, direct use of air or O_2 as a cathodic oxidant in such a liquid flow fuel cell is usually of low efficiency. Using POM liquid catalyst such as $H_3PMo_{12}O_{40}$ (Zhao and Zhu, 2016) and $H_{12}P_3Mo_{18}V_7O_{85}$ (Liu et al., 2014a,b) could greatly improve the power density. In the present work, a much cheaper liquid catalyst, i.e. Fe^{3+}, was used as an electron carrier in cathode. More importantly, the reduced product of Fe^{3+}, namely Fe^{2+} is very easy to re-oxidize by air or oxygen.

The cell reactions can be simply expressed as Eqs. (7)–(9) when Fe^{3+} is used as an electron mediator in cathode (Zhao et al., 2016):

$$\text{Anode half}-\text{cell reaction}: Mo^{5+} \rightarrow Mo^{6+} + e^-,\ E^{\Theta} = 0.50V \quad (7)$$

(Bard et al., 1985)

$$\text{Cathode half}-\text{cell reaction}: Fe^{3+} + e^- \rightarrow Fe^{2+},\ E^{\Theta} = 0.77V \quad (8)$$

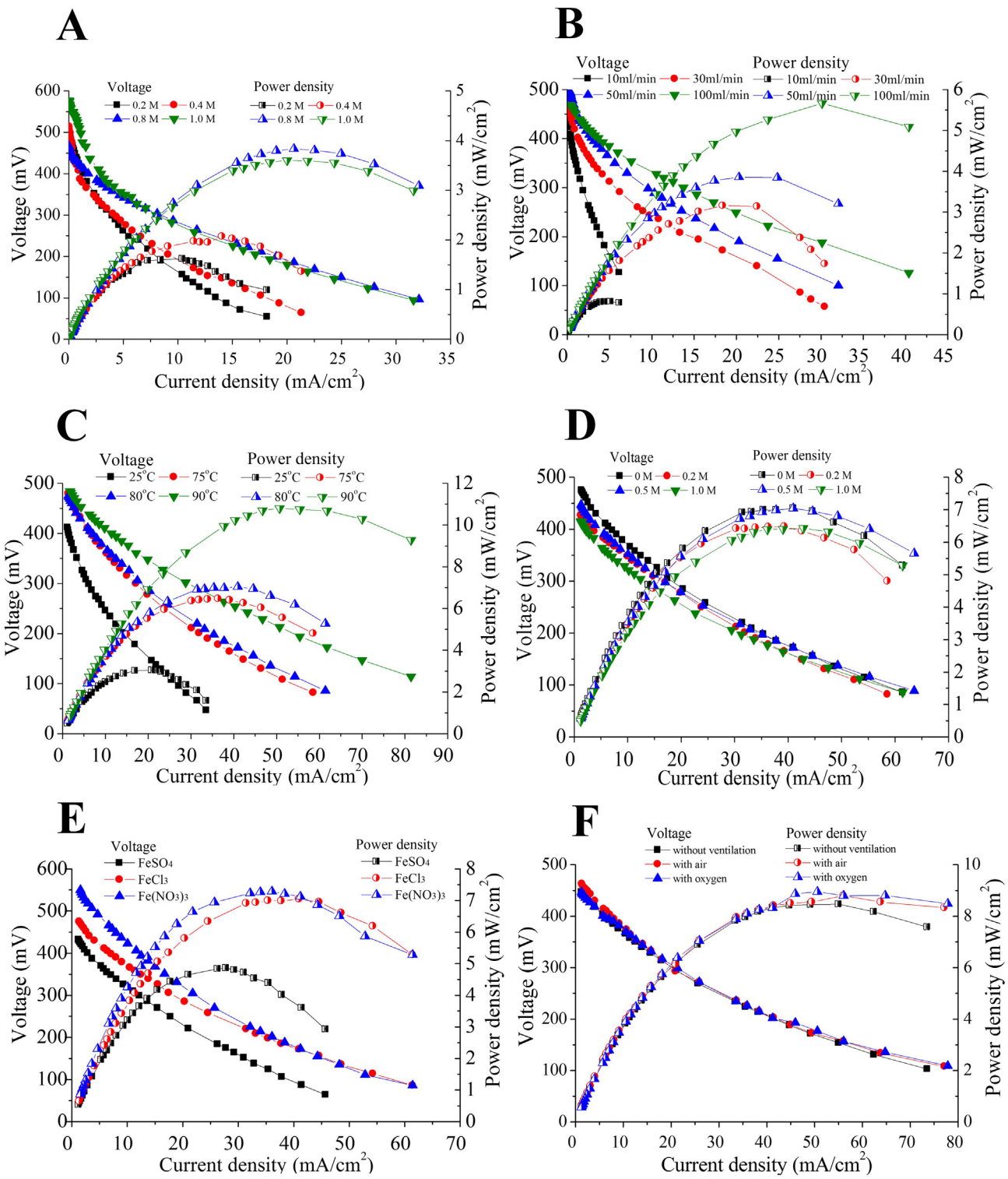

Fig. 4. Effects of various factors on discharging of reduced PMo_{12}. (A) Effects of $FeCl_3$ concentration at 70 °C with 1.5 cm^2 electrode active area; (B) Effects of flowrate with 3.12 cm^2 electrode active area; (C) Effects of temperature with 0.7 cm^2 electrode active area; (D) Effects of H^+ concentration in cathode solution at 80 °C with 0.7 cm^2 electrode active area; (E) Effects of different ferric salts 80 °C with 0.7 cm^2 electrode active area; (F) Effects of ventilation with air or oxygen at gas flow rate of 10 ml/min.

$$\text{Total cell reaction}: Mo^{5+} + Fe^{3+} \rightarrow Mo^{6+} + Fe^{2+}, E^{\Theta}_{mf} = 0.77 - 0.50 = 0.27V \quad (9)$$

The Nernst equation of the total cell potential (E_{TC}) is:

$$E_{TC} = E^{\Theta}_{mf} - \frac{RT}{F} \ln \frac{[Fe^{2+}][Mo^{6+}]}{[Fe^{3+}][Mo^{5+}]} \quad (10)$$

Eq. (10) indicates that the cell potential is influenced by reaction temperature, ratio of $[Fe^{3+}]$ to $[Fe^{2+}]$ and $[Mo^{6+}]$ to $[Mo^{5+}]$. Increasing temperature, Mo^{5+} concentration in anode solution and Fe^{3+} concentration in cathode solution is beneficial to enhancing cell potential. As shown in Fig. 4A, $FeCl_3$ concentration indeed showed a significant effect on power density of the cell. The P_{max}s were 1.62, 1.97, 3.84 and 3.60 mW/cm^2 at $FeCl_3$ concentration of

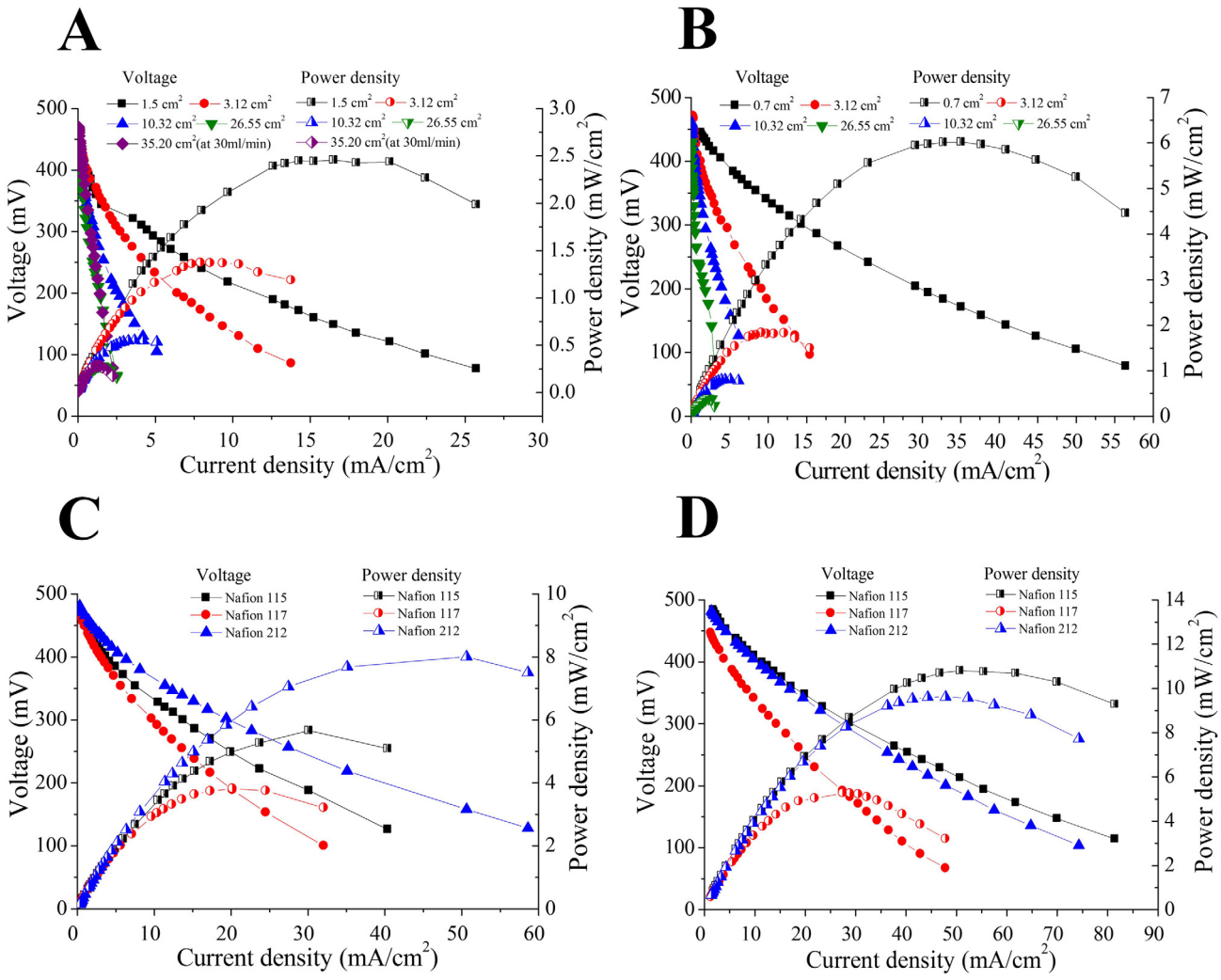

Fig. 5. Effects of several structural factors of the cell on discharging of reduced PMo_{12}. (A) Effects of active area at 60 °C; (B) Effects of active area at 75 °C; (C) Effects of PEM type with active area of 0.7 cm^2; (D) Effects of PEM type with active area of 3.12 cm^2.

0.2, 0.4, 0.8 and 1.0 M, respectively. Corresponding open circuit voltages (OCVs) were determined in the range of 0.47–0.58 V. Flow rate also showed a significant impact on the power output. As shown in Fig. 4B, the power density increased with temperature, and the highest P_{max} reached 5.66 mW/cm^2 at a flowrate of 100 ml/min (the maximum flow rate of the pump used). It was probably because that increasing flow rate could facilitate the contact between the solution and electrodes (graphite bipolar plate) to accelerate electron transfer. However, more importantly, as we found in the experiments, increasing flow rate could make the temperature of the cell chamber closer to that in the external vessel. For example, when a cell with electrode active area (EAA) of 3.12 cm^2 was used in the experiments, the temperature of cell chamber increased from 75 °C at 10 ml/min flow rate to 90 °C at 100 ml/min when the external vessels were kept at 95 °C. Therefore, the effects of temperature on discharging were further investigated at a constant flow rate (100 ml/min). As shown in Fig. 4C, power density was dramatically improved as temperature increased. A P_{max} of 11 mW/cm^2 with OCV of 510 mV could be obtained at 90 °C of cell chamber temperature. Addition of external H^+ in cathode solution did not improve the power density as shown if Fig. 4D. This is reasonable because H^+ is not involved in the cell reactions as shown in Eqs. (7)–(9). Contrarily addition of 1 M H^+ (as HCl) somewhat decreased P_{max}. This might be due to the decrease of proton concentration difference between anode and cathode chambers which reduced the proton transfer across the PEM. However, it should be noted that H^+ take part in the reaction of re-oxidation of Fe^{2+} to Fe^{3+} by oxygen as shown in Eq. (5). Therefore, addition of some external H^+ might be beneficial to the regeneration of Fe^{3+} by ventilation of air or oxygen in cathode vessel.

Ferric salt species also showed significant impacts on discharging at the same Fe^{3+} concentration (0.8 M), as shown in Fig. 4E (Zhao et al., 2016). $Fe(NO_3)_3$ obtained the highest power density (7.29 mW/cm^{-2}) followed by $FeCl_3$ (7.04 mW/cm^{-2}), while $Fe_2(SO_4)_3$ showed the poorest power output (4.86 mW/cm^{-2}). However, when $Fe(NO_3)_3$ was used, NO_3^- played as an oxidant and took part in the cathodic reaction with formation of some derivative products. Therefore, it is not a suitable electron mediator for discharging, and $FeCl_3$ is the most promising candidate.

As aforementioned, ventilation of air or oxygen in cathode vessel to re-oxidize Fe^{2+} to Fe^{3+} might improve the power output. As shown in Fig. 4F, P_{max} indeed was somewhat improved by ventilation of air or oxygen, with P_{max} increased from 8.47 mW/cm^2 to 8.80 mW/cm^2 with air and 8.95 mW/cm^2 with oxygen, respectively. After discharging for 3 h, the Fe^{2+} concentration in cathode vessel was 0.50 M, compared with 0.37 M with ventilation of air and 0.32 M with oxygen, respectively. It indicated that by continuously ventilating air, the power density indeed could be improved, and electron could be finally transferred to oxygen. However, as

found in the experiments, in a continuous operation of a cell with 50 ml anode and cathode solution at EAA of 0.7 cm^2 and 35.2 cm^2 and respectively, $I_{2\Omega}$ deceased from 74 and 167 mA at the beginning of discharging to 55 and 94 mA, respectively, after 3 h operation, even if biomass fuel was fed every 1 h. This reduction of power output was because that the rates of "charging" (pretreatment) and re-oxidation of Fe^{2+} by air was lower than that the "discharging" (re-oxidation of PMo_{12} in the cell). Therefore, the pretreatment (charging process), re-oxidation of Fe^{2+} by air and ratio of electrode solution volume to EAA have to be further intensified and optimized to improve the stability of power output.

3.2.2. Effects of cell structural factors

Cell structures such as electrode active area (EAA) and PEM type are also important factors affecting the power output. As shown in Fig. 5A and B, EAA demonstrated very significant impacts on power and current density. At 60 °C, as EAA increased from 1.5 cm^2 to 35.2 cm^2, P_{max} decreased from 2.45 to 0.28 mW/cm^2 while $I_{2\Omega}$ (output current at external loading of 2 Ω) increased from 38.6 mA to 65.0 mA. At 75 °C, P_{max} decreased from 6.02 to 0.39 mW/cm^2 with $I_{2\Omega}$ increasing from 39.5 to 71.0 mA. This result indicated that small EAA could obtain high power density, while large EAA was beneficial to achieving high output current. PEM is another important structural factor influencing electricity generation. Three commercial PEMs, namely Nafion®115, Nafion®117 and Nafion®212 were compared as shown in Fig. 5C and D. These PEMs have different thickness (212–50 μm, 115–127 μm and 117–183 μm, respectively) with different resistance. The thinnest PEM (212) showed the highest P_{max} (8.00 mW/cm) at a relative small EAA (3.12 cm^2), while the thickest PEM (117) showed the lowest (3.82 mW/cm^2). However, at a small EAA (0.7 cm^2), Nafion®115 and Nafion®212 demonstrated similar P_{max} (9.62 and 10.80 mW/cm^2, respectively), while Nafion®117 showed much lower P_{max} (5.26 mW/cm^2). Therefore, Nafion®212 is a preferred PEM for PMo_{12} regeneration and electricity generation in the liquid flow fuel cell. By determining the changes of *RD* in anode solution and Fe^{2+} concentration in cathode solution after discharging for 3 h (without ventilating air into the cathode vessel), the Faradaic efficiency was calculated to be as high as 97%.

The above results corroborated that PMo_{12} is a good candidate for mediating biomass pretreatment and electricity generation. This is majorly attributed to the special properties of PMo_{12}. PMo_{12} has acidity and thus can promote the hydrolysis of hemicelluloses and cleavage of lignin intramolecular linkage for fragmentation. PMo_{12} also has strong oxidation ability to degrade lignin. Compared with commonly used oxidants such as H_2O_2 and hypochlorous acid, PMo_{12} can be easily regenerated and recycled, and the re-oxidation of reduced PMo_{12} in a liquid flow fuel cell (or redox flow cell) indeed generates electricity simultaneously as demonstrated in the present work. Moreover, in the present work, Fe^{3+} was used as a mediator in cathode, which is much cheaper than POM as a candidate for mediating electron transfer (Zhao et al., 2016). More importantly, the Fe^{3+} can be easily regenerated by oxidation of the Fe^{2+} at low temperature using air or oxygen. By optimizing the operation parameters and cell structures, a highest P_{max} of about 11 mW/cm^2 were obtained. However, it should be noted that the cell device used in this work was just a simple one, and the electrode used was just graphite bipolar plate. The power density would be further improved by more parameter optimization and cell structure development, especially the electrode material.

3.3. Mass balance of the integrated process

Based on the above experimental results, a mass balance for the integrated process can be made as shown in Fig. 6. After pretreatment, 60% of the wheat straw was recovered as solid phase, with a cellulose recovery of 78% and *DD* of 61%. 69% of xylan was also solubilized during pretreatment. When the pretreated substrates was used for fermentable sugar production by enzymatic hydrolysis, 22.5 g glucose plus 5.4 g xylose could be obtained from 100 g raw wheat straw, corresponding to 58.3% and 21.0% of theoretical glucose and xylose yields from wheat straw. After fermentation, ethanol yield of 11 g/100 g wheat straw was obtained, corresponding to 55.8% of theoretical yield from the raw feedstock. The used PMo_{12} concentration (0.20–0.25 M) was much higher than conventional dilute acid pretreatment (typically less than 0.1 M), in order to achieve a good power output in the liquid flow fuel cell.

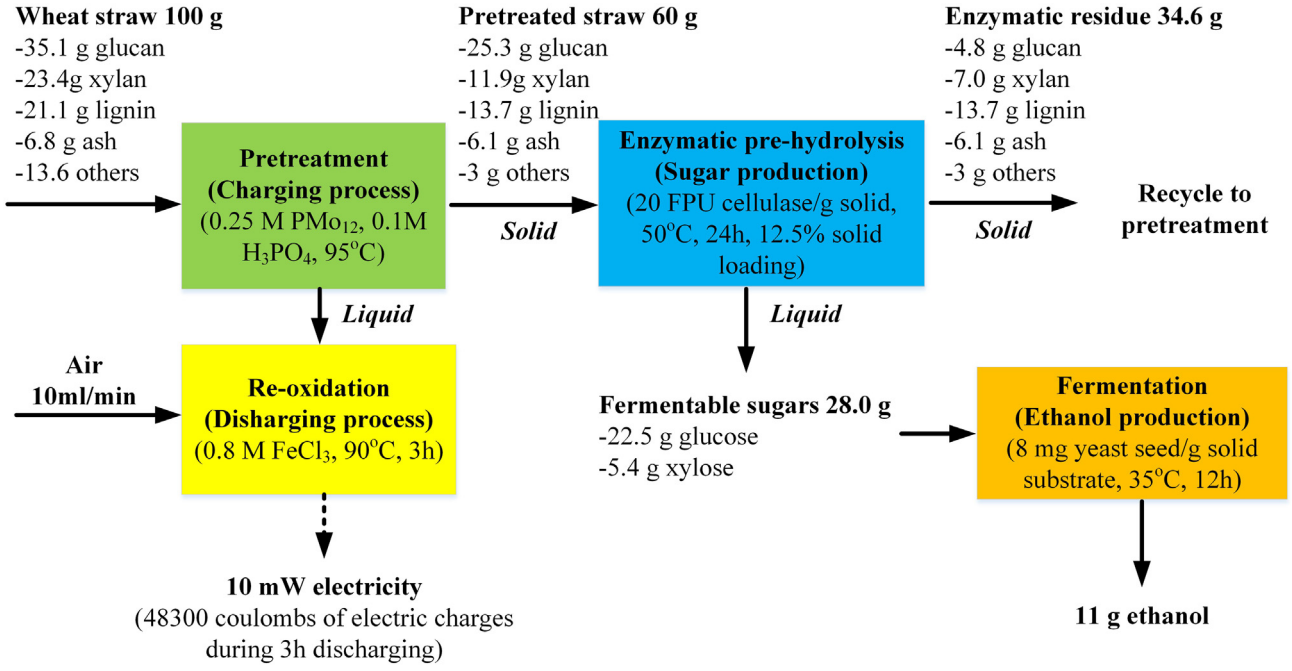

Fig. 6. Mass balance of the integrated process for ethanol production and electricity generation.

However, the solubilized fraction and hydrolyzate also can be oxidized by PMo_{12} to yield PMo_{12red}. 10 mW electricity corresponding to transfer of 48,300 coulombs of electric charges was obtained. In the experiments, when an external resistance load was 2Ω, the average current during discharging was about 100 mA, thus the energy capacity obtained was about 300 mAh for the liquid flow cell.

Although this integrated process can achieve a co-production of ethanol and electricity generation, there is still a great space to improve the efficiency. In an ideal scenario, cellulose and hemicellulose are converted to sugars while lignin to electricity. Theoretically, from 100 g of wheat straw used in this work, 38.6 g glucose, 25.7 g xylose and 21.1 g lignin could be obtained. If the lignin is completed oxidized to CO_2 and water, there would be about 3.6 mol electrons transferring to the oxidant, corresponding to 350 000 coulombs of electric charges. However, in this work, the ethanol yield was 11 g per 100 g wheat straw with transfer of 48,300 coulombs of electric charges as shown in the mass balance calculation. The relatively low ethanol yield was mainly due to the solubilization of polysaccharides during PMo_{12} pretreatment, causing loss of sugars for fermentation. However the hydrolyzate may be also oxidized by PMO_{12} (Sarma and Neumann, 2014), which contributed to electricity generation. The efficiency of lignin-to-electricity was not high enough mainly because under the pretreatment condition some lignin structure cannot be oxidized by PMo_{12} (Zhao and Zhu, 2016).

It also should be noted that in the experiments, the pretreated substrates must be washed with water or even with ethanol and ether to recover most of the PMo_{12} and remove the residual PMo_{12} in the pretreated solid, because PMo_{12} as an acid and oxidant is detrimental to enzymatic hydrolysis and fermentation of pretreated substrates. However, using solvent for washing would increase the pretreatment cost, though the volatile solvents can be easily recovered by evaporation. Compared with conventional pretreatment process such as dilute acid hydrolysis and steam explosion, this pretreatment would be too expensive. However, in a large-scale process, multi-stage counter-current water washing can be used to recover PMo_{12} and remove its residue in the pretreated solid as proposed by Weinstock et al. (1996) for environmentally-benign bleaching of kraft pulp. An external wet oxidation of not fully-discharged PMo_{12red} can be performed at higher temperature and under O_2 pressure, in which the dissolved organic compounds can be converted completely to CO_2 to reduce COD of the effluent (Weinstock et al., 1996). Therefore, to further improve the efficiency of the process, more works should be done to study the kinetics of the pretreatment process, the dynamics of the discharging, developing cell apparatus as well as process design and energy efficiency analysis. A carbon element mass balance also should be done to trace the "carbon footprint" of this integrated process.

4. Conclusion

PMo_{12} and ferric iron are good mediators to achieve an integration of biomass pretreatment for ethanol production and efficient conversion of biomass components, especially lignin, to electricity. Significant solubilization of polysaccharide and condensation of lignin were observed at pretreatment temperature higher than 140 °C, while the highest cellulose enzymatic digestibility was obtained at 100–120 °C. The reduced PMo_{12} could be well re-oxidized in a liquid flow fuel cell with generation of electricity simultaneously. $FeCl_3$ was an effective liquid mediator to transfer electrons to air, with a P_{max} of about 11 mW/cm^2 under the optimal discharging conditions.

Acknowledgement

Authors are grateful to National Natural Science Foundation of China (No. 21106081, No. 21406130), National Energy Administration Project (No. NY20130402) and Dongguan Social and Technical Development Project (No. 2015108101004) for supporting this work.

Appendix A. Supplementary data

Supplementary data associated with this article can be found, in the online version, at http://dx.doi.org/10.1016/j.biortech.2016.12.109.

References

Akimkulova, A., Zhou, Y., Zhao, X.B., Liu, D.H., 2016. Improving the enzymatic hydrolysis of dilute acid pretreated wheat straw by metal ion blocking of non-productive cellulase adsorption on lignin. Bioresour. Technol. 208, 110–116.
Amirabedin, E., McIlveen-Wright, D.A., 2013. Feasibility study of co-firing biomass in the thermal power plant at soma in order to reduce emissions: an exergy approach. Int. J. Environ. Res. 7, 139–154.
Bard, A., Parsons, R., Jordan, J., 1985. Standard Potentials in Aqueous Solution. CRC Press, p. 480.
Bujanovic, B., Ralph, S., Reiner, R., Hirth, K., Atalla, R., 2010. Polyoxometalates in oxidative delignification of chemical pulps: effect on lignin. Materials 3, 1888–1903.
Chen, H.M., Zhao, J., Hu, T.H., Zhao, X.B., Liu, D.H., 2015. A comparison of several organosolv pretreatments for improving the enzymatic hydrolysis of wheat straw: Substrate digestibility, fermentability and structural features. Appl. Energy 150, 224–232.
Chen, H.M., Zhao, X.B., Liu, D.H., 2016. Relative significance of the negative impacts of hemicelluloses on enzymatic cellulose hydrolysis is dependent on lignin content: evidence from substrate structural features and protein adsorption. ACS Sustainable Chem. Eng. 4, 6668–6679.
Ding, S.Y., Liu, Y.S., Zeng, Y., Himmel, M.E., Baker, J.O., Bayer, E.A., 2012. How does plant cell wall nanoscale architecture correlate with enzymatic digestibility? Science 338, 1055–1060.
Donohoe, B., Decker, S., Tucker, M., Himmel, M., Vinzant, T., 2008. Visualizing lignin coalescence and migration through maize cell walls following thermochemical pretreatment. Biotechnol. Bioeng. 101, 913–925.
Gaspar, A., Evtuguin, D.V., Neto, C.P., 2003. Oxygen bleaching of kraft pulp catalysed by Mn(III)-substituted polyoxometalates. Appl. Catal., A 239, 157–168.
Gaspar, A., Gamelas, J., Evtuguin, D., Neto, C., 2007. Alternatives for lignocellulosic pulp delignification using polyoxometalates and oxygen: a review. Green Chem. 9, 717–730.
Katsoulis, D.E., 1998. A survey of applications of polyoxometalates. Chem. Rev. 98, 359–387.
Kim, J.S., Lee, Y.Y., Kim, T.H., 2016. A review on alkaline pretreatment technology for bioconversion of lignocellulosic biomass. Bioresour. Technol. 199, 42–48.
Kim, S.B., Lee, J.H., Oh, K.K., Lee, S.J., Lee, J.Y., Kim, J.S., Kim, S.W., 2011. Dilute acid pretreatment of barley straw and its saccharification and fermentation. Biotechnol. Bioprocess. Eng. 16, 725–732.
Kim, W.B., Voitl, T., Rodriguez-Rivera, G.J., Dumesic, J.A., 2004. Powering fuel cells with CO via aqueous polyoxometalates and gold catalysts. Science 305, 1280–1283.
Kozhevnikov, I.V., 1998. Catalysis by heteropoly acids and multicomponent polyoxometalates in liquid-phase reactions. Chem. Rev. 98, 171–198.
Liu, W., Mu, W., Deng, Y.L., 2014b. High-performance liquid-catalyst fuel cell for direct biomass-into-electricity conversion. Angew. Chem. Int. Ed. 53, 13558–13562.
Liu, W., Mu, W., Liu, M., Zhang, X., Cai, H., Deng, Y., 2014a. Solar-induced direct biomass-to-electricity hybrid fuel cell using polyoxometalates as photocatalyst and charge carrier. Nat. Commun. 5, 3208.
Lynd, L.R., 1996. Overview and evaluation of fuel ethanol from cellulosic biomass: Technology, economics, the environment, and policy. Annu. Rev. Energy Environ. 21, 403–465.
Morikawa, Y., Zhao, X.B., Liu, D.H., 2014. Biological co-production of ethanol and biodiesel from wheat straw: a case of dilute acid pretreatment. RSC Adv. 4, 37878–37888.
Saha, B., Iten, L., Cotta, M., Wu, Y., 2005. Dilute acid pretreatment, enzymatic saccharification and fermentation of wheat straw to ethanol. Process Biochem. 40, 3693–3700.
Sarma, B.B., Neumann, R., 2014. Polyoxometalate-mediated electron transfer-oxygen transfer oxidation of cellulose and hemicellulose to synthesis gas. Nat. Commun. 5, 4621.
Singh, R., Shukla, A., Tiwari, S., Srivastava, M., 2014. A review on delignification of lignocellulosic biomass for enhancement of ethanol production potential. Renewable Sustainable Energy Rev. 32, 713–728.

Tamura, H., Goto, K., Yotsuyanagi, T., Nagayama, M., 1974. Spectrophotometric determination of iron(II) with 1,10-phenanthroline in the presence of large amounts of iron(III). Talanta 21, 314–318.

Weinstock, I.A., Atalla, R.H., Reiner, R.S., Moen, M.A., Hammel, K.E., Houtman, C.J., Hill L, C., 1996. A new environmentally benign technology and approach to bleaching kraft pulp. Polyoxometalates for selective delignification and waste mineralization. New J. Chem. 20, 269–275.

Wu, W.B., Liu, W., Mu, W., Deng, Y.L., 2016. Polyoxymetalate liquid-catalyzed polyol fuel cell and the related photoelectrochemical reaction mechanism study. J. Power Sources 318, 86–92.

Zeng, Y., Zhao, S., Yang, S., Ding, S.Y., 2014. Lignin plays a negative role in the biochemical process for producing lignocellulosic biofuels. Curr. Opin. Biotechnol. 27, 38–45.

Zhang, H., Wu, T., Yan, X., Leng, Y., Li, S., 1990. The redox characteristics of molybdophosphoric heteropolyacids, molybdovanadophosphoric heteropolyacids and their salts. Chem. J. Chin. Univ. 11, 1096–1101.

Zhao, X.B., Zhu, J.Y., 2016. Efficient conversion of lignin to electricity using a novel direct biomass fuel cell mediated by polyoxometalates at low temperatures. Chemsuschem 9, 197–207.

Zhao, X.B., Cheng, K.K., Liu, D.H., 2009. Organosolv pretreatment of lignocellulosic biomass for enzymatic hydrolysis. Appl. Microbiol. Biotechnol. 82, 815–827.

Zhao, X.B., Zhang, L.H., Liu, D.H., 2012a. Biomass recalcitrance. Part I: the chemical compositions and physical structures affecting the enzymatic hydrolysis of lignocellulose. Biofuels Bioprod. Biorefin. 6, 465–482.

Zhao, X.B., Zhang, L.H., Liu, D.H., 2012b. Biomass recalcitrance. Part II: Fundamentals of different pre-treatments to increase the enzymatic digestibility of lignocellulose. Biofuels Bioprod. Biorefin. 6, 561–579.

Zhao, X.B., Ding, Y., Du, B., Liu, D.H., 2016. Polyoxometalate-mediated lignin oxidation for efficient enzymatic production of sugars and generation of electricity from lignocellulosic biomass. Energy Technol. http://dx.doi.org/10.1002/ente.201600662.

Zhou, Y., Chen, H.M., Qi, F., Zhao, X.B., Liu, D.H., 2015. Non-ionic surfactants do not consistently improve the enzymatic hydrolysis of pure cellulose. Bioresour. Technol. 182, 136–143.

Zhu, J.Y., Pan, X.J., Wang, G.S., Gleisner, R., 2009. Sulfite pretreatment (SPORL) for robust enzymatic saccharification of spruce and red pine. Bioresour. Technol. 100, 2411–2418.

Zhu, J., Pan, X., 2010. Woody biomass pretreatment for cellulosic ethanol production: Technology and energy consumption evaluation. Bioresour. Technol. 101, 4992–5002.